



A Sahlberg et al.

## Propagating Transport-code input parameter uncertainties with Deterministic Sampling

Preprint of Paper to be submitted for publication in  
Plasma Physics and Controlled Fusion



This work has been carried out within the framework of the EUROfusion Consortium and has received funding from the Euratom research and training programme 2014-2018 under grant agreement No 633053. The views and opinions expressed herein do not necessarily reflect those of the European Commission.

This document is intended for publication in the open literature. It is made available on the clear understanding that it may not be further circulated and extracts or references may not be published prior to publication of the original when applicable, or without the consent of the Publications Officer, EUROfusion Programme Management Unit, Culham Science Centre, Abingdon, Oxon, OX14 3DB, UK or e-mail Publications.Officer@euro-fusion.org

Enquiries about Copyright and reproduction should be addressed to the Publications Officer, EUROfusion Programme Management Unit, Culham Science Centre, Abingdon, Oxon, OX14 3DB, UK or e-mail Publications.Officer@euro-fusion.org

The contents of this preprint and all other EUROfusion Preprints, Reports and Conference Papers are available to view online free at <http://www.euro-fusionscipub.org>. This site has full search facilities and e-mail alert options. In the JET specific papers the diagrams contained within the PDFs on this site are hyperlinked

# Propagating Transport-code input parameter uncertainties with Deterministic Sampling

*A. Sahlberg<sup>1</sup>, C. Hellesen<sup>1</sup>, J. Ericsson<sup>1</sup>, S. Conroy<sup>1</sup>,  
G. Ericsson<sup>1</sup>, D. King<sup>2</sup> and JET Contributors<sup>3</sup>*

<sup>1</sup>*Dept. of Physics and astronomy, Uppsala University, Sweden*

<sup>2</sup>*CCFE, Culham Science Centre, Abingdon, Oxfordshire, UK*

<sup>3</sup>*See the author list of "X. Litaudon et al 2017 Nucl. Fusion 57 102001"*

## Abstract

A novel approach to uncertainty quantification in codes simulating fusion plasma, Deterministic Sampling (DS), is evaluated. This method uses a few carefully selected samples and can be used to propagate input parameter uncertainties through calculations where other sampling methods are unmanageable due to time constraints. The primary analysis is performed on the transport code TRANSP, but another faster code is also tested where a comparison with Monte Carlo sampling is made.

The tests, performed with two JET pulses, show that even lower order DS will give a reliable estimation of the standard deviation of the calculated neutron rate. However, a higher order DS can give information about higher output moments, such as skewness and kurtosis. The TRANSP-simulated neutron rates of both examined pulses are found to have an uncertainty with an upward skewness, meaning input parameter uncertainties can better explain an underestimation of the neutron rate than an overestimation. This information can, for example, be used to lead to a better benchmarking comparison between the measured and calculated neutron rates.

## 1 Introduction

A commonly used method for modeling fusion plasma properties, such as fuel ion distributions[1] confinement time[2], or diamagnetic flux[3], is the transport code TRANSP[4], developed at Princeton Plasma Physics Laboratory. It is often used together with the code NUBEAM[5] which models the slowing down of the beam ions.

When conducting TRANSP simulations, an agreement between the calculated and the measured neutron rate is frequently used as validation of a TRANSP run's accuracy[6][7]. However, a challenge with such a comparison is the difficulty in knowing how much deviation between the measured and calculated neutron rate is acceptable. This question is one example of the need for

rigorous uncertainty quantification in TRANSP, as well as transport codes and simulations in general.

Usually, when any simulation is performed, the input parameters come from a measurement. In most measurements, an estimation of the uncertainty exists, yet in other cases the uncertainty is unknown. In any case, one wants to estimate the uncertainty of the simulation's result, either by propagating the known input uncertainty or by assuming a worst reasonable case. Either way, the uncertainty of the input parameters have to be propagated through the calculation.

There are many approaches to uncertainty quantification, and a significant class of such is sampling methods, such as Monte Carlo methods. Here the input parameters are sampled randomly many times, and the propagated uncertainty can be calculated from the result of the simulation being performed with each of those samples. In the standard Monte Carlo method many samples, often a few hundred or even a few thousand, are needed for a reliable estimation of the propagated uncertainty. Sometimes running hundreds of simulations is not a problem, but with massive and time-consuming simulations, this many samples can make Monte Carlo methods unreasonable to use due to high time cost.

The high time cost of Monte Carlo can be circumvented in various ways. One way is to use Stratified Sampling or Latin-Hypercube Sampling[8], which are techniques to divide the parameter-space into smaller areas and sample those individually. Another way is to work with surrogate models[9], meant to approximate the original model with one which can be evaluated much faster. Building a surrogate model though is not trivial and can be time-consuming in itself.

In 1995[10] Uhlman defined the Unscented Transform (UT) based on the idea that *it is easier to approximate a probability distribution function than it is to approximate an arbitrary model*. UT approximates a continuous probability distribution with a set of weighted samples which encode the lowest order statistical moments. The simulation is performed with each sample and from the results, the propagated uncertainty is calculated.

Unscented Transform has traditionally been used in signal processing[11] and Kalman filters[12]. In more recent years UT has found uses for uncertainty propagation in the other fields, for example, wind turbine simulations[13], power flow[14], state estimation[15][16], magnetic field mapping[17], battery capacity assessment[18] and CFD computations in nuclear reactors[19]. To the authors best knowledge, Unscented Transform has not been applied to fusion reactor simulations until now.

UT has also been re-branded as Deterministic Sampling[20] (DS). This name may be more explanatory, given that, for one, the method uses deterministically calculated samples rather than a randomized ensemble, and secondly, it does not involve an actual transformation without loss of information but instead makes an approximation of the input parameters' distribution.

This paper evaluates the application of DS for uncertainty propagation in TRANSP. The uncertainty in the electron temperature, ion temperature, electron density and Z-effective have been propagated through TRANSP calculations, and the resulting uncertainty in the neutron rate has been determined.

The expectation value, the standard deviation, the skewness and the kurtosis of the uncertainty in the neutron rate have been calculated and compared to the measured value.

When evaluating the usefulness of DS, the best case would be to compare it to Monte Carlo. While this can not be done with TRANSP, due to time-consuming simulations, a comparison between DS and Monte Carlo has been made on the code TRAP-T[21], which executes fast enough for Monte Carlo to be applicable.

## 2 Deterministic Sampling

Deterministic Sampling (or Unscented Transform) propagates uncertainty through a function or simulation by running it with a small set of sigma-points, called an ensemble. The sigma-points are chosen to represent the uncertain input parameters' probability distributions well. The sigma-points  $q^{(i)}$  each have a weight  $w^{(i)}$  associated with them, and usually the weights are normalized so that  $\sum w^{(i)} = 1$ . This way the ensemble can be seen as a discrete approximation of the probability distribution it represents. In figure 1 this discrete approximation can be seen for a one-dimensional probability distribution.

In practice, the sigma-points are found by letting the ensemble encode the same lowest order statistical moments as the uncertain input parameters' distributions. In the simple case of only one uncertain input parameter  $Q$ , with a known probability distribution  $f(Q)$ , the ensemble  $\{w^{(i)}, q^{(i)}\}$  representing this would be one which has the same the expectation value and variance, i.e.

$$\langle Q \rangle = \int_{-\infty}^{\infty} f(Q) dQ = \sum_i w^{(i)} q^{(i)}, \quad (2.1)$$

$$\text{var}(Q) = \int_{-\infty}^{\infty} (f(Q) - \langle Q \rangle)^2 dQ = \sum_i w^{(i)} (q^{(i)} - \langle Q \rangle)^2. \quad (2.2)$$

Encoding only two moments is the lowest order form of DS, but is still widely used in uncertainty quantification[13][22][23]. To reach a higher order of accuracy, one needs to include more moments in the ensemble. Usually adding the third and fourth moments is considered enough. Encoding the skewness and kurtosis is done by letting the sigma-points fulfill

$$\text{skw}(Q) = \int_{-\infty}^{\infty} \frac{(f(Q) - \langle Q \rangle)^3}{\text{var}(Q)^{3/2}} dQ = \sum_i \frac{w^{(i)} (q^{(i)} - \langle Q \rangle)^3}{\text{var}(Q)^{3/2}} \quad (2.3)$$

$$\text{kur}(Q) = \int_{-\infty}^{\infty} \frac{(f(Q) - \langle Q \rangle)^4}{\text{var}(Q)^2} dQ = \sum_i \frac{w^{(i)} (q^{(i)} - \langle Q \rangle)^4}{\text{var}(Q)^2}. \quad (2.4)$$

This can in principle be done with any number of moments encoded, but a larger number of moments will usually mean a larger and harder to find ensemble.

Usually a simulation has more than one uncertain input parameter, and in this case, their correlations need to be encoded as well.

Once the sigma-points are found the simulation is run with each sigma-point, producing a set of output samples  $S(q^{(i)})$ . From those, the uncertainty of the result is calculated. The expectation value and variance of the result are estimated as

$$\langle S(Q) \rangle = \sum_i w^{(i)} S(q^{(i)}) \quad (2.5)$$

$$\text{var}(S(Q)) = \sum_i w^{(i)} \left( S(q^{(i)}) - \langle S(Q) \rangle \right)^2. \quad (2.6)$$

Higher order moments of the result can be calculated with corresponding expressions.

In short process of DS is as follows. For the uncertain input parameters, a set of sigma-points is chosen to represent the first few moments of their probability distributions. Once this ensemble has been determined, the process is the same as in a Monte Carlo method, i.e., the simulation is run with each of the samples giving a set of transformed sigma-points. From the simulation's output, the resulting uncertainty is calculated.

The validity of this approach has been argued for by using Taylor expansions[24], or by invoking the correctness of ensuring the statistical knowledge available is encoded in the samples[20].

The process is illustrated with an example in figure 1. Here the uncertainty of a random normal distributed variable  $Q$  with  $\mu = 2$  and  $\sigma = 0.5$  is propagated through a non-linear function  $f(Q) = Q^3$ . The process is shown using ensembles encoding two moments and six moments and the samples are shown before and after the function is applied. One can see that the higher moment ensemble captures the behavior better than the two-moment one. The values gained from the uncertainty propagation with Deterministic Sampling, using two, four and six input-moments in the ensemble, are compared to that gained by Monte Carlo in table 1.

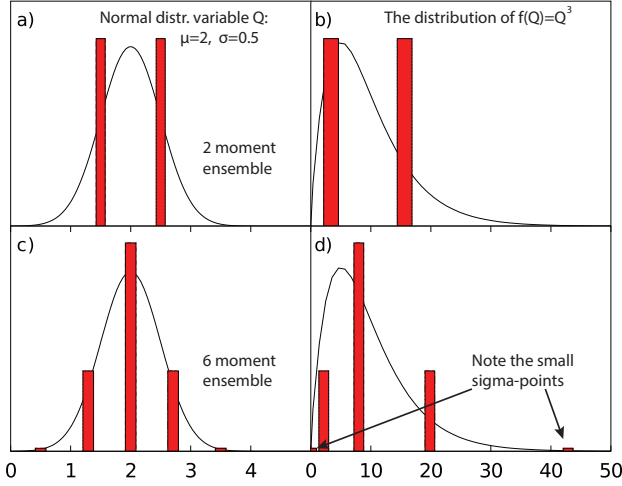


Fig. 1: The Gaussian distribution of a random variable  $Q$ , along with a two-moment ensemble **a**) and a six-moment ensemble **c**) for DS. **b**) and **d**) shows  $f(Q) = Q^3$  for the same variable, along with the propagated samples. Two-moment ensemble from **a**) and **b**) only gives information about mean value and standard deviation, but the higher order ensemble from **c**) and **d**) gives information about higher moments, e.g. skewness and kurtosis, as well.

Tab. 1: The estimated uncertainty from DS using ensembles of two, four and six input moments when propagating the uncertainty of a random normal distributed variable  $Q$  with  $\mu = 2$  and  $\sigma = 0.5$  through the function  $f(Q) = Q^3$ .

	Mean value	St. dev.	Skewness	Kurtosis	Num. samples
2 moments	9.50	6.125	0.0	1.0	2
4 moments	9.50	6.718	1.23	3.52	3
6 moments	9.50	6.726	1.44	6.34	5
Monte Carlo	9.501(5)	6.723(6)	1.440(4)	6.25(27)	10000

From table 1 one can see that including more input-moments in the ensemble one will get a better estimation of the output uncertainty. Specifically, the higher output moments, skewness and kurtosis, needs higher input-moments for a good result.

For a more in-depth explanation of Deterministic Sampling Hessling's paper[20] is suggested.

To verify the accuracy of the uncertainty gained from Deterministic Sampling, one has to compare the propagated uncertainty with some reference value. This comparison can be made using the result of some other method of uncer-

tainty quantification, for example, Monte Carlo. In this paper, we also use a less rigorous form of verification which benchmarks DS against itself by comparing with DS simulations using a higher number of encoded moments. For example, if DS with two moments agrees with DS with four moments, it is an indication that using two moments are enough.

### 3 Method

In this study, the uncertainty in the input parameters is propagated through TRANSP simulations, and the uncertainty of the calculated neutron rate is determined with Deterministic Sampling. The four input parameters used are the electron density ( $n_e$ ), electron temperature ( $T_e$ ), ion temperature ( $T_i$ ) and effective plasma charge ( $Z_{\text{eff}}$ ), since TRANSP relies heavily on these parameters.

The TRANSP uncertainty quantifications have been done with two different JET pulses. As described in 3.2, DS has also been applied to TRAP-T[21] which calculates the 14 MeV neutron emission rate from a JET pulse and evaluates fast enough so that a comparison with Monte Carlo methods is viable.

The JET pulses used with TRANSP are 86918, a pulse with high neutron rate, no RF heating and a neutron emission dominated by neutrons from beam-target reactions and 92436, currently the highest neutron rate in an ILW plasma with a neutron rate dominated by neutrons from thermonuclear reactions. TRAP-T is run with an older pulse, 51009. A summary of the shots is shown in Table 2.

Tab. 2: Properties of the analyzed JET pulses.

Pulse	$B_T$	$I_p$	$n_e$	$T_e$	$P_{\text{NBI}}$	$P_{\text{ICRH}}$	Code
86918	2.1 T	2.0 MA	$6.5 \times 10^{19} \text{ m}^{-3}$	4 keV	18 MW	0	TRANSP
92436	2.8 T	3.0 MA	$8 \times 10^{19} \text{ m}^{-3}$	6 keV	27.2 MW	6.0 MW	TRANSP
51009	2.6 T	2.5 MA	$3 \times 10^{19} \text{ m}^{-3}$	8 keV	7.6 MW	3.6 MW	TRAP-T

#### 3.1 The TRANSP simulations

The TRANSP simulations for shot 86918 has been run in the time interval 7 s to 14 s and the ones for 92436 are run in the interval 8 s to 13 s. The measured values of these parameters are shown in Figure 2, along with the neutron rate and the NBI-heating power. The temperature and density have, in the plot, been sliced at the magnetic axis. In the actual simulations, full profile data has been used. Both the TRANSP and measured neutron rate is shown. These TRANSP simulations are run with the unperturbed measured values for all the parameters.

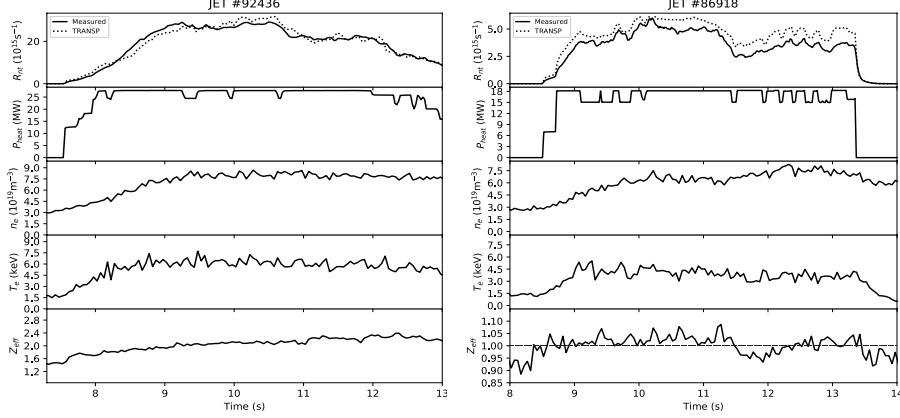


Fig. 2: Measurements of the electron density, electron temperature and  $Z_{\text{eff}}$  on the magnetic axis, along with the total heating power and both measured and simulated neutron rate for pulse 92436 (left) and 86918 (right).

Measurements of  $n_e$  and  $T_e$  have been done with High-Resolution Thompson Scattering[25] (HRTS) for pulse 86918 and with Light Detection and Ranging (LIDAR) Thompson scattering[26] for 92436. The ion temperature  $T_i$  has been handled differently for the two pulses. For 92436 the ion temperature has been measured with charge exchange recombination spectroscopy[27]. For 86918 the measurement of  $T_e$  has been used as ion temperature, but it is treated as an independent  $T_i$  measurement.

These three parameters are all assumed to be normally distributed with a sigma of 5%. For  $Z_{\text{eff}}$  the line averaged value measured by the visible bremsstrahlung diagnostic KS3 is used, and its sigma is assumed to be 10%. Note that the uncertainties assumed here may not depict the actual diagnostic uncertainty. They are more of a rough estimation of what the uncertainties are expected to be for these parameters. If we were to go forward with this method in the future, a more detailed investigation of what the diagnostic uncertainties are has to be made. For the current paper where the aim is to assess the usefulness of this method, we assume stated uncertainties.

As seen in Figure 2, the measured  $Z_{\text{eff}}$  for pulse 86918 is below one for much of the time interval. That an effective plasma charge lower than one is unphysical follows directly from its definition[28], and hence the actual value must be one or higher.

The measured value of  $Z_{\text{eff}}$  is assumed to have a Gaussian uncertainty and to be constant during the simulation. The average value of the measurements over the discharge, here 0.99, is used as the mean value and the standard deviation is assumed to be 10%. The non-physical measurement is treated in the same Bayesian manner as, for example, the unphysical measurement of the neutrino

mass[29]. The uncertainty distribution from the measured value  $f_{\text{meas}}(Z_{\text{eff}})$  is multiplied with a prior which eliminates the non-physical region. Then the distribution is renormalized, and the posterior distribution is found. This way the skewed distribution of  $Z_{\text{eff}}$  is constructed, and it is shown in figure 3.

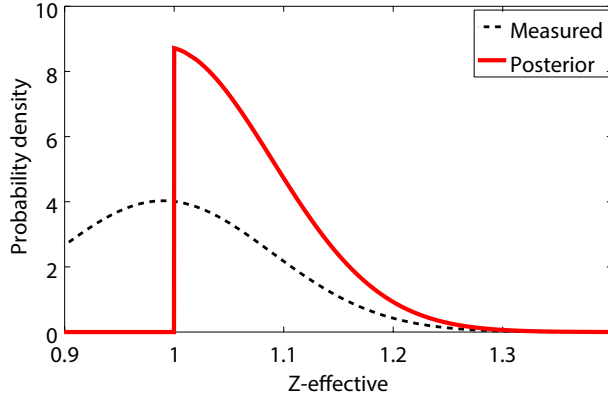


Fig. 3: The probability distribution of  $Z_{\text{eff}}$  for pulse 86918, i.e. the positive part of a normal distribution centred at 0.99.

Together these uncertain parameters have a four-dimensional distribution. For this distribution, three ensembles have been created, encoding the first two, four and six moments. These ensembles have been used to propagate these uncertainties to the simulated neutron rate in TRANSP.

### 3.2 TRAP-T uncertainty and Monte Carlo comparison

To make a comparison between Deterministic Sampling and Monte Carlo, Deterministic Sampling has been applied to TRAP-T[21], another code for calculating neutron emissions. This code, which calculates the 14 MeV neutron emission from a JET pulse, has been investigated similarly as TRANSP, i.e., input parameter uncertainties have been propagated to the calculated neutron rate with DS. This code has the advantage of executing fast enough for Monte Carlo methods to be useful and hence the DS result can be compared to an MC value.

The test with TRAP-T has been run with JET pulse 51009 in the time interval 6 s to 13 s. The parameters used for uncertainty propagation are  $n_e$ ,  $n_i$ ,  $T_e$ ,  $T_i$ , and  $Z_{\text{eff}}$  and the uncertainty of the 14 MeV neutron rate is calculated. All these parameters are assumed to have a Gaussian uncertainty with a sigma of 10 %. Deterministic Sampling has been run with ensembles encoding two, four and six moments and the result has been compared with a Monte Carlo test using 10,000 samples. The comparison has been made for the uncertainty in the neutron emission rate at a single time step in the code.

### 3.3 Validation

Two forms of validating the results have been used here. First, the TRAP-T uncertainty propagation is compared with the uncertainty estimated by Monte Carlo. Second, the Deterministic Sampling has been compared to itself using a higher order of accuracy. The uncertainty propagation has been performed with three different ensembles encoding two, four and six moments, and the results have been compared. For the uncertainty of the resulting neutron rate, the first four moments have been calculated. The resulting uncertainty given by the three different ensembles have been compared, and outcomes that agree with the six-moment results are considered reliable.

### 3.4 Analysis

A TRANSP simulation has been run with each sigma-point in each ensemble. From the resulting neutron rates an expectation value, variance, skewness, and kurtosis, representing the uncertainty of the result, have been calculated. The different values for those gained from the three different ensembles have been compared.

If one performs uncertainty quantification with Monte Carlo, one gets a complete distribution of the result. However, Deterministic Sampling only gives information about the lowest order moments of the output. Given this, it may still be interesting to estimate what the distribution is like, if not for any other reason than to visualize the meaning of a particular skewness and kurtosis. To visualize the meaning of the four calculated moments, a probability distribution function has been fitted to these moments using the technique described below in section 3.4.1. This is done for both the total neutron rate as well as the thermonuclear and beam-target neutron rate components.

#### 3.4.1 Fitting a PDF to higher order output moments

If we only have information about the two lowest moments, i.e., expectation value and standard deviation, the assumption to make would be to see the output variable as a Gaussian (normal) distribution. If we, however, have information about four moments, i.e., about skewness and kurtosis as well, a normal distribution can not encode this information. In this case, a modified version of the normal distribution is here used to encode both a non-zero skewness and non-Gaussian kurtosis.

To encode the third moment we use a modified version of the Gaussian distribution, what Hosking[30] calls the *Lognormal distribution* (not the usual the Lognormal distribution). Encoding kurtosis in a normal distribution can be done with what Nadarajah[31] calls the *Generalised Normal Distribution*. Combining Hosking's Lognormal distribution and Nadarajah's Generalized Normal Distribution we find the following expression for a continuous PDF,

$$f(x) = \frac{g(y(x, \xi, \kappa, \alpha), \beta)}{\alpha - \kappa(x - \xi)} \quad (3.1)$$

where

$$y(x, \xi, \kappa, \alpha) = \begin{cases} -\frac{1}{\kappa} \log \left( 1 - \frac{\kappa(x-\xi)}{\alpha} \right), & k \neq 0 \\ \frac{x-\xi}{\alpha}, & k = 0. \end{cases} \quad (3.2)$$

and

$$g(x, \beta) = \frac{\beta}{2\sqrt{2}\Gamma(1/\beta)} \exp \left[ -\left| \frac{x}{\sqrt{2}} \right|^\beta \right] \quad (3.3)$$

giving us a possibility to adjust the kurtosis with  $\beta$ , the skewness with  $\kappa$ , set the variance with  $\alpha$  and the mean value with  $\xi$ . The parameters in (3.1) can be fitted to encode the first four moments given from the output given from the use of Deterministic Sampling.

## 4 Results and discussion

### 4.1 TRAP-T

From the uncertainty of the five parameters used in the TRAP-T simulations and the application of Deterministic Sampling, the expectation value, the standard deviation, the skewness and the kurtosis of the 14 MeV neutron rate has been calculated. The same thing has been calculated with Monte Carlo simulations for comparison.

The mean values and standard deviations gained by Deterministic Sampling ensembles agree well with the Monte Carlo values. Even the lowest order two-moment ensemble give a reliable estimation of the resulting parameter uncertainty. Since the standard deviation often is what one is looking for when one does an uncertainty analysis, using a two-moment ensemble can be enough.

Higher order moments, skewness and kurtosis, are calculated here as well. The calculated positive skewness of the result is captured by all the ensembles, although the six-moment ensemble gets it most accurate. The resulting kurtosis is the hardest one to get right, and only the six-moment ensemble shows a good agreement with the Monte Carlo value.

From the calculated mean, standard deviation, skewness, and kurtosis of the neutron rate, the estimated distribution of the neutron rate uncertainty has been constructed using (3.1). Such a distribution has been determined from both the values given by the Deterministic Sampling and Monte Carlo, and they are presented at one time-slice in figure 4.

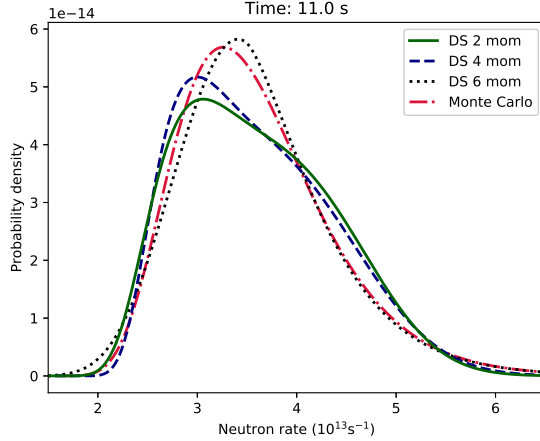


Fig. 4: The 14 MeV neutron rate distribution of JET pulse 51009 reconstructed from uncertainty quantification with both Deterministic Sampling and Monte Carlo.

Note that even in the ensemble which only inserts two moments, a value for higher-moments can be calculated, although should not be trusted. This is in contrast to the example shown in figure 1 and table 1 where the two-moment ensemble only used two samples and hence no skewness or kurtosis could be found. In this case where there are four parameters the number of samples is high enough to calculate a non-trustworthy value of the uncertainty's skewness and kurtosis.

This test indicates that Deterministic Sampling can produce reliable results for neutron rate uncertainty estimation, comparable to Monte Carlo methods. As previously stated, in the TRANSP simulations Monte Carlo cannot be used due to time constraints. Instead, the results from the two, four and six-moment ensembles are compared with each other, where the six-moment ensemble is considered most reliable.

## 4.2 TRANSP

As an example of the data an ensemble produces, the neutron rates from the TRANSP simulations of the six-moment ensemble of pulse 86918 is plotted in figure 5. Each curve represents the neutron rate from a simulation with one sigma-point from the ensemble, and the line-widths symbolize their various weights.

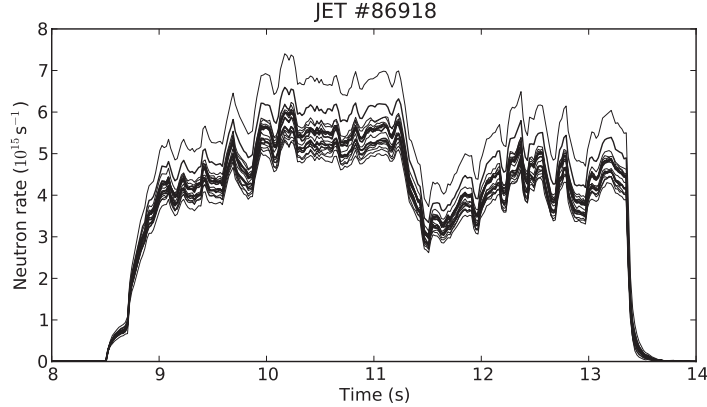


Fig. 5: The TRANSP simulations for the six-moment Deterministic Sampling uncertainty quantification of pulse 86918.

From the simulations with each ensemble, as shown in figure 5, the mean value, standard deviation, skewness, and kurtosis of the neutron rate has been calculated using equation (2.5) and (2.6). The time-traces of the resulting moments are shown in figure 6 for both pulses.

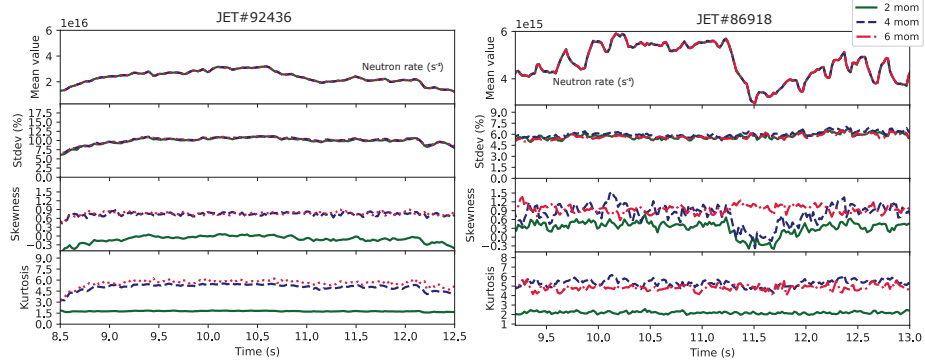


Fig. 6: The time trace of the resulting neutron rate mean value, standard deviation, skewness and kurtosis for pulse 92436 (left) and 86918 (right).

A good agreement between all the three DS runs is found for the mean value and standard deviation. Regarding skewness and kurtosis, two moments are not sufficient to get a good value, which is expected. The four and six-moment ensembles mostly agree, both indicating a skewness around 1, and a kurtosis around 5 for pulse 86918 and slightly lower values for 92436.

As the 86918 neutron rate drops at 51.2 s, so does the skewness of the two and four moment runs, while the six-moment runs' skewness stays roughly the

same throughout the whole run. The four-moment skewness seems to fluctuate more than the six-moment runs, but beside the dip, at 51.2 seconds it appears to get the correct value on average.

To get an estimation of the mean value and standard deviation, an ensemble encoding the first two moments is enough and often when performing uncertainty quantification an assessment of the standard deviation is what one is after. The yellow region in figures 7 and 8 represents the 67% confidence interval, which corresponds to one sigma, which is usually plotted as error bars. However, showing the impact of higher moments can be necessary when determining whether a discrepancy between calculated and simulated neutron rate is significant.

As described in section 4.1, a neutron rate distribution is reconstructed from the four output moments at each time-slice. The distribution is an approximation that fulfills the four lowest order moments gained from an uncertainty propagation carried out with a limited number of input moments. However, even knowing this is an approximation, it can be seen as an indication of in which region the actual value should be, given the calculated moments of the output uncertainty.

The fitted neutron rate uncertainty distribution for the pulses is shown in figure 7. The 67% 95% and 99% confidence intervals are showed in different colors. This distribution is shown for both the total neutron rate as well as for the beam-target and thermonuclear neutron rates for both pulse 92436 and 86918.

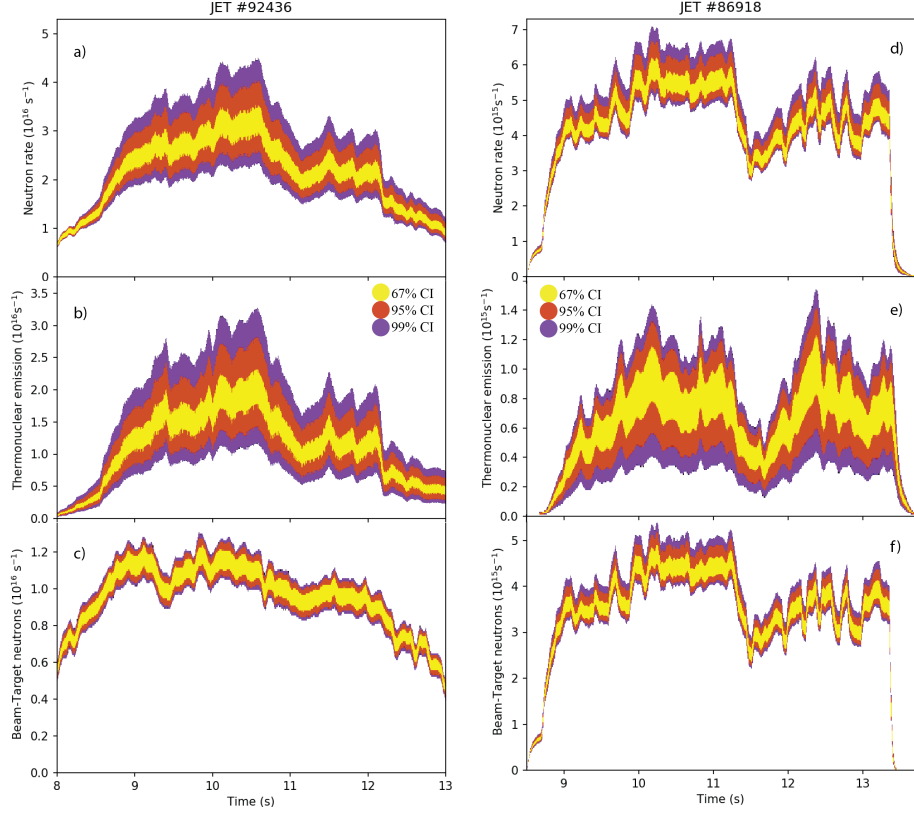


Fig. 7: The simulated neutron rate uncertainty for both the total neutron rate (top), thermonuclear neutron rate (middle) and Beam-Target neutron rate (bottom) for pulses 92436 (left) and 86918 (right).

By visualizing the uncertainty, as shown in figure 7, one can make a better comparison with the measured neutron rate, rather than just making a visual comparison as in the top of figure 2. Figure 8 demonstrates this by displaying the measured neutron rate together with the estimated uncertainty of the simulated TRANSP neutron rate.

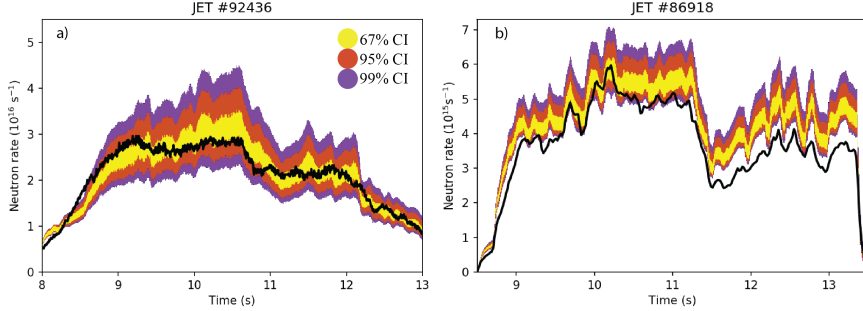


Fig. 8: The calculated uncertainty of the simulated neutron rate compared to the measured neutron rate for both pulse 92436 (a) and 86918 (b).

Both investigated pulses show a neutron rate uncertainty with a positive skewness, as seen in figure 8. If the simulation has an uncertainty skewed upwards, one can conclude that a downward deviation from the measured value can be tolerable and could still be considered a match. On the other hand, an upward deviation of the same magnitude, as seen in figure 8b, means the simulation is indeed not compatible with the measurements.

The discrepancy shown in 8b after 11 s is, because of the upward skewness, significant and can not be explained by the input uncertainties (assuming we have not underestimated them). Had the measured neutron rate been above the simulated by the same amount, the match would still be questionable, but not impossible. This result further corroborates the result presented in [32] where it was concluded that input parameter uncertainties do not explain the systematic modeled neutron overproduction at JET.

When addressing the modeled overproduction of neutrons (sometimes referred to as a 'neutron deficit'), it is important to remember what is meant by this positive skewness. The interpretation of the TRANSP neutron rate uncertainty is that it shows which deviations from the measured neutron rate values can be explained by the given input parameter uncertainties, as is illustrated in figure 9a. In other words, the PDF gives a degree of compatibility between the measured and the simulated neutron rates.

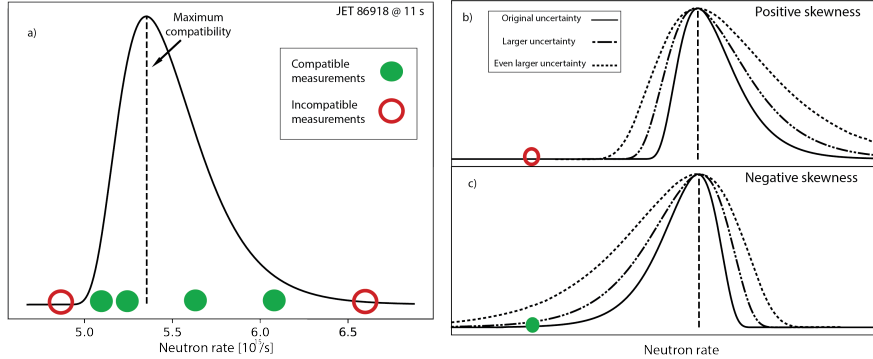


Fig. 9: a) The TRANSP neutron rate uncertainty of pulse 86918 at 11 s, showing which measured neutron rates can be considered to agree with the TRANSP simulation. The positive skewness means a measured neutron rate higher than the TRANSP value is more tolerable than a downward deviation. b) The positive skewness means even if the magnitude of the uncertainty is increased, it would be hard to explain a significantly lower measured than modeled neutron rate. If on the other hand, as in c), there was a negative skewness it would help explain the modeled overproduction of neutrons.

TRANSP will often produce a 0-100% higher neutron rate than what is measured at JET[32], and this is hard to explain by uncertainties alone, even with more substantial input parameter uncertainties than the ones used in this paper. The positive skewness means the compatibility with lower neutron rates is worse than it had been with a Gaussian distribution. Even if the uncertainty were broader than shown here, the upward skewness would hinder the distribution from reaching the much lower values, as displayed in figure 9b. Had there been a negative skewness instead, as shown in 9c, it would have helped to explain the lower measured neutron rate, but this result shows the opposite case.

In addition to the estimated skewness, the kurtosis will impact our estimation of whether the simulated and measured neutron rates match. Kurtosis can tell us how likely extreme deviations from the expectation value are. If kurtosis is high, as in for example figure 7b, where the yellow 67% confidence interval is small compared to the other, deviations from the mean value greater than one sigma are not unlikely. If, on the other hand, kurtosis is small, as in figure 7c a deviation of just two standard deviations is entirely unreasonable.

According to the tests performed here, information about the skewness and kurtosis of the result is reliable, which is indicated by the agreement between the four and six-moment ensembles (as seen in figure 6). Hence if one is interested in the higher moments of the neutron rate uncertainty, an ensemble including four moments is sufficient.

Here the uncertainty propagating has been examined assuming a 5% sigma in  $n_e$ ,  $T_e$  and  $T_i$ , which may be an underestimation for some of the used diagnostics and an overestimation for others. Regardless of this, DS should be a valid method of propagating uncertainty even with smaller or larger uncertainties.

Another assumption made is that the uncertainties in the input parameters are independent, and hence the covariance is zero. Uncorrelated parameter-uncertainties are expected if they are measured independently, but that is not necessarily the case here. For example, both  $n_e$  and  $T_e$  are measured by the same instrument and therefore we should expect some correlation between their uncertainties. A covariance can be encoded into the ensembles, and its effect on the resulting uncertainty studied, but this has not been done here.

## 5 Conclusions

Based on the tests performed in this paper we draw the conclusions that, Deterministic Sampling produces reliable results and give a sound estimation of the simulation's uncertainty when applied to either of the tested codes TRAP-T or TRANSP. For these codes, the method gives a consistent estimate of the neutron rate error, and when a comparison with Monte Carlo has been possible, results have agreed.

Apart from producing a reliable estimate of the neutron rate standard deviation, information about the third and fourth order moments can also be obtained, if their input-parameter counterparts are included in the simulation. In other words, when Deterministic Sampling is applied to TRANSP using samples which encode a skewness and kurtosis of the input-parameters, the estimated skewness and kurtosis of the simulated neutron rate are consistent. Such a description of the neutron rate distribution can, for example, be used for more precise comparison between the simulated and measured neutron rates when benchmarking TRANSP runs.

The four output moments have been used to produce an approximated distribution function of the TRANSP neutron rate uncertainty, which can be used as a degree of compatibility between the modeled and the measured neutron rates, for benchmarking purposes. Because of its positive skewness, a TRANSP simulation's deviation from a significantly lower measured neutron rate is made less acceptable than if the distribution would have been Gaussian, or if the skewness would have been negative.

Only two pulses have been investigated in this paper, one dominated by thermonuclear reactions and one by beam-target reactions. While the magnitude of their neutron rate uncertainties differs one has a sigma of 6% and one has almost twice as high, they both have an upward skewness, meaning the simulated neutron rate in those two pulses is more likely to underestimate the actual neutron rate than to overestimate it. This upward skewness means that there is a difference between whether the simulation diverges upwards or downwards from the measured neutron rate. In especially one of the tested pulses it can be seen that downward deviation of two sigmas can still be seen as a match,

while an upward deviation of the same amount is significantly outside the region which can be explained by input parameter uncertainties.

Both pulses also have a high kurtosis of five to six, compared to the normal distribution's kurtosis of three. Since both have a similar shape, it is an interesting question whether this is a general shape of the TRANSP neutron rate uncertainty or these just happened to be similar by coincidence.

In this paper, Deterministic Sampling has been applied to two fusion related codes and is found to perform well. It can be utilized for uncertainty propagation in other transport codes as well and could be valuable as a quicker alternative to Monte Carlo methods when a high computational time is an issue.

### **Acknowledgement**

This work has been carried out within the framework of the EUROfusion Consortium and has received funding from the Euratom research and training programme 2014-2018 under grant agreement No 633053. The views and opinions expressed herein do not necessarily reflect those of the European Commission.

## References

- [1] C. Hellesen, E. A. Sundén, S. Conroy, G. Ericsson, L. Giacomelli, A. Hjalmarsson, M. G. Johnsson, J. Källne, E. Ronchi, M. Weiszflog, L. Ballabio, G. Gorini, M. Tardocchi, I. Voitsekhovitch, and J.-E. Contributors, “Validating TRANSP simulations using neutron emission spectroscopy with dual sight lines,” *Review of Scientific Instruments*, vol. 79, p. 10E510, oct 2008.
- [2] I. Chapman, M.-D. Hua, S. Pinches, R. Akers, A. Field, J. Graves, R. Hastie, C. Michael, and t. M. Team, “Saturated ideal modes in advanced tokamak regimes in MAST,” *Nuclear Fusion*, vol. 50, p. 045007, apr 2010.
- [3] L. Giannone, B. Geiger, R. Bilato, M. Maraschek, T. Odstrčil, R. Fischer, J. C. Fuchs, P. J. McCarthy, V. Mertens, and K. H. Schuhbeck, “Real-time diamagnetic flux measurements on ASDEX Upgrade,” *Review of Scientific Instruments*, vol. 87, p. 053509, may 2016.
- [4] R. J. Goldston, D. C. McCune, H. H. Towner, S. L. Davis, R. J. Hawryluk, and G. L. Schmidt, “New techniques for calculating heat and particle source rates due to neutral beam injection in axisymmetric tokamaks,” *Journal of Computational Physics*, vol. 43, no. 1, pp. 61–78, 1981.
- [5] A. Pankin, D. McCune, R. Andre, G. Bateman, and A. Kritz, “The tokamak Monte Carlo fast ion module NUBEAM in the national transport code collaboration library,” *Computer Physics Communications*, vol. 159, no. 3, pp. 157–184, 2004.
- [6] I. Klimek, M. Cecconello, M. Gorelenkova, D. Keeling, A. Meakins, O. Jones, R. Akers, I. Lupelli, M. Turnyanskiy, G. Ericsson, and t. M. Team, “TRANSP modelling of total and local neutron emission on MAST,” *Nuclear Fusion*, vol. 55, p. 023003, feb 2015.
- [7] S. Gerhardt, E. Fredrickson, D. Gates, S. Kaye, J. Menard, M. Bell, R. Bell, B. Le Blanc, H. Kugel, S. Sabbagh, and H. Yuh, “Calculation of the non-inductive current profile in high-performance NSTX plasmas,” *Nuclear Fusion*, vol. 51, p. 033004, mar 2011.
- [8] M. D. McKay, R. J. Beckman, and W. J. Conover, “A Comparison of Three Methods for Selecting Values of Input Variables in the Analysis of Output from a Computer Code,” *Technometrics*, vol. 21, p. 239, may 1979.
- [9] G. Kurz and U. D. Hanebeck, “Deterministic Sampling on the Torus for Bivariate Circular Estimation,” *IEEE Transactions on Aerospace and Electronic Systems*, vol. 53, no. 1, pp. 530–534, 2017.
- [10] Uhlmann Jeffrey K., “Dynamic map building and localization for autonomous vehicles,” 1995.

- [11] R. Amara, "Improving Parallel EKF-based nonlinear channel equalization using unscented transformation," *Network*, pp. 304–324, 2004.
- [12] P. Li, T. Zhang, and B. Ma, "Unscented Kalman filter for visual curve tracking," *Image and Vision Computing*, vol. 22, no. 2, pp. 157–164, 2004.
- [13] R. Khorramnia, M.-R. Akbarizadeh, M. K. Jahromi, S. K. Khorrami, and F. Kavusifard, "A new unscented transform for considering wind turbine uncertainty in ED problem based on SSO algorithm," *Journal of Intelligent & Fuzzy Systems*, vol. 29, no. 4, pp. 1479–1491, 2015.
- [14] H. R. Baghaee, M. Mirsalim, G. B. Gharehpetian, and H. A. Talebi, "Fuzzy unscented transform for uncertainty quantification of correlated wind/PV microgrids: possibilistic–probabilistic power flow based on RBFNNs," *IET Renewable Power Generation*, vol. 11, pp. 867–877, may 2017.
- [15] S. Wang, W. Gao, and A. P. S. Meliopoulos, "An Alternative Method for Power System Dynamic State Estimation Based on Unscented Transform," *IEEE Transactions on Power Systems*, vol. 27, pp. 942–950, may 2012.
- [16] S. Chun, H.-M. Choi, B.-R. Yoon, and W. Kang, "Implementation of unscented transform to estimate the uncertainty of a liquid flow standard system," *Journal of Mechanical Science and Technology*, vol. 31, pp. 1189–1194, mar 2017.
- [17] P. Arpaia, E. De Matteis, and R. Schiano Lo Moriello, "Unscented transform-based uncertainty analysis of rotating coil transducers for field mapping," *Review of Scientific Instruments*, vol. 87, p. 035004, mar 2016.
- [18] W. Zhang, W. Shi, and Z. Ma, "Adaptive unscented Kalman filter based state of energy and power capability estimation approach for lithium-ion battery," *Journal of Power Sources*, vol. 289, pp. 50–62, sep 2015.
- [19] P. Hedberg, P. Hessling, and M. Technology, "Use of Deterministic Sampling for Uncertainty Quantification in Cfd," *Nureth-16*, pp. 4907–4920, 2015.
- [20] J. P. Hessling, "Deterministic Sampling for Propagating Model Covariance," *SIAM/ASA Journal Uncertainty Quantification*, vol. 1, pp. 297–318, 2013.
- [21] S. Conroy, O. Jarvis, G. Sadler, and G. Huxtable, "Time resolved measurements of triton burnup in JET plasmas," *Nuclear Fusion*, vol. 28, no. 12, p. 2127, 1988.
- [22] M. T. Nasri and W. Kinsner, "Extended and unscented Kalman filters for the identification of uncertainties in a process," in *2013 IEEE 12th International Conference on Cognitive Informatics and Cognitive Computing*, pp. 182–188, IEEE, jul 2013.

- [23] G. Valverde and V. Terzija, "Unscented Kalman filter for power system dynamic state estimation," *IET Generation, Transmission & Distribution*, vol. 5, no. 1, p. 29, 2011.
- [24] S. Julier and J. Uhlmann, "Unscented Filtering and Non Linear Estimation," *Proceedings of the IEEE*, vol. 92, no. 3, pp. 401–422, 2004.
- [25] R. Pasqualotto, P. Nielsen, C. Gowers, M. Beurskens, M. Kempenaars, T. Carlstrom, and D. Johnson, "High resolution Thomson scattering for Joint European Torus (JET)," *Review of Scientific Instruments*, vol. 75, no. 10 II, pp. 3891–3893, 2004.
- [26] M. Maslov, M. N. Beurskens, M. Kempenaars, and J. Flanagan, "Status of the JET LIDAR Thomson scattering diagnostic," *Journal of Instrumentation*, vol. 8, no. 11, 2013.
- [27] A. Boileau, M. V. Hellermann, L. D. Horton, J. Spence, and H. P. Summers, "The deduction of low-Z ion temperature and densities in the JET tokamak using charge exchange recombination spectroscopy," *Plasma Physics and Controlled Fusion*, vol. 31, pp. 779–804, may 1989.
- [28] S. K. Rathgeber, R. Fischer, S. Fietz, J. Hobirk, A. Kallenbach, H. Meister, T. Pütterich, F. Ryter, G. Tardini, and E. Wolfrum, "Estimation of profiles of the effective ion charge at ASDEX Upgrade with Integrated Data Analysis," *Plasma Physics and Controlled Fusion*, vol. 52, no. 9, 2010.
- [29] V. N. Aseev, A. I. Belesev, A. I. Berlev, E. V. Geraskin, A. A. Golubev, N. A. Likhovid, V. M. Lobashev, A. A. Nozik, V. S. Pantuev, V. I. Parfenov, A. K. Skasyrskaya, F. V. Tkachov, and S. V. Zadorozhny, "Upper limit on the electron antineutrino mass from the Troitsk experiment," *Physical Review D - Particles, Fields, Gravitation and Cosmology*, vol. 84, no. 11, 2011.
- [30] J. R. M. Hosking and J. R. Wallis, "Appendix: L-moments for some specific distributions," in *Regional frequency analysis: an approach based on L-moments*, pp. 191–209, Cambridge: Cambridge University Press.
- [31] S. Nadarajah, "A generalized normal distribution," *Journal of Applied Statistics*, vol. 32, no. 7, pp. 685–694, 2005.
- [32] H. Weisen, H.-T. Kim, J. Strachan, S. Scott, Y. Baranov, J. Buchanan, M. Fitzgerald, D. Keeling, D. King, L. Giacomelli, T. Koskela, M. Weisen, C. Giroud, M. Maslov, W. Core, K.-D. Zastrow, D. Syme, S. Popovichev, S. Conroy, I. Lengar, L. Snoj, P. Batistoni, M. Santala, and J. Contributors, "The 'neutron deficit' in the JET tokamak," *Nuclear Fusion*, vol. 57, p. 076029, jul 2017.